Low-Energy-Barrier Proton Transfer Induced by Electron Attachment to the Guanine···Cytosine Base Pair

ARTICLE *in* CHEMPHYSCHEM · MARCH 2010

Impact Factor: 3.42 · DOI: 10.1002/cphc.200900810 · Source: PubMed

7 AUTHORS, INCLUDING:

Janusz Rak
University of Gdansk
145 PUBLICATIONS **2,132** CITATIONS
SEE PROFILE

Xiang li
Johns Hopkins University
42 PUBLICATIONS **518** CITATIONS
SEE PROFILE

Kit H Bowen
Johns Hopkins University
240 PUBLICATIONS **5,909** CITATIONS
SEE PROFILE

CHEMPHYSCHEM

DOI: 10.1002/cphc.200900810

Low-Energy-Barrier Proton Transfer Induced by Electron Attachment to the Guanine···Cytosine Base Pair

Anna Szyperska,[a] Janusz Rak,*[a] Jerzy Leszczynski,*[b] Xiang Li,[c] Yeon Jae Ko,[c] Haopeng Wang,[c] and Kit H. Bowen*[c]

The photoelectron spectrum of the anion of the guanine···cytosine base apair $(GC)^{\bullet-}$ is recorded for the first time. The observed variation in the spectral peak-height ratios with the source conditions suggests the presence of two or more anionic isomers. Two maxima of the broad bands in the photoelectron spectrum were measured at about 1.9 and about 2.6 eV. These values are very well reproduced by the vertical detachment energies of the B3LYP/6-31++G(d,p) calculated low-energy anionic structures, which are 1) the Watson–Crick base-pair anion with proton transferred from N1 of guanine to N3 of cytosine, 2) its analogue in which the proton is transferred from N9 of guanine to N7 of guanine, and 3) the global minimum geometry, which is formed from the latter anion by rotation of guanine about the axis approximately defined by C2 of guanine and C4 of cytosine. Furthermore, a minor difference in the stabilities of the two lowest energy anions explains the experimentally observed source (temperature) dependence of the PES spectrum. A rational procedure, based on the chemistry involved in the formation of anionic dimers, which enables the low-energy anions populated in the photoelectron spectrum to be identified is proposed. In contrast to the alternative combinatorial approach, which in the studied case would lead to carrying out quantum chemical calculations for 2000–2500 structures, the procedure described here reduces the computational problem to only 15 geometries.

1. Introduction

As early as 1962, Eley and Spivey[1] suggested that the unique DNA π stack may serve as a medium for charge transfer in this fundamental biopolymer. Currently, this remarkable DNA feature seems to be well documented through many experiments, which range from time-resolved spectroscopic measurements[2–4] to biochemical assays.[5–8] The vital consequences of this phenomenon for biology and nanotechnology have not yet been completely comprehended, and current studies focus on these aspects rather than on acquiring further evidence for its existence. The biological implications of long-distance charge transfer in DNA have both negative and positive aspects as far as the integrity of the DNA molecule is concerned. For instance, it was demonstrated[9] that rhodium complexes (a hole source) tethered covalently to DNA fragments are able to photodamage guanine residues that are separated by many base pairs from the intercalation site. On the other hand, long-distance hole transfer was shown to be involved in the repair of thymine photodimer that was as far as as 26 Å from the rhodium catalyst.[10] Several genes have GC-rich sequences outside of the encoding area[11] that act as a protective sink for the positive charge, so that mutations occur in the nonencoding area of DNA even if the hole was originally generated in the coding sequence of a gene.

Electron transport in DNA is also interesting from the technological point of view.[12–14] Nowadays, the demand for more powerful computational devices is satisfied through miniaturization of silicon-based chips (the top-down approach). However, the alternative bottom-up procedure could be based on the synthesis of molecules having suiatble features which could then be assembled into electronic devices. To this end, the ability of DNA to transfer electrons over long distances offers an attractive possibility to use oligonucleotides in nanotechnological applications as relatively cheap and self-organizing nanowires.

While oxidative DNA damage through long-range DNA charge transfer (CT) has been studied extensively,[15–18] less attention has been devoted to studying DNA reduction.[19–24] Demand for this type of investigations emerged after the discovery by Sanche et al. of DNA damage by low-energy electrons. By irradiation of plasmid DNA deposited on a tantalum surface with an electron beam of controlled energy, they demonstrated unequivocally that these electrons with energies

[a] A. Szyperska, Prof. J. Rak
Department of Chemistry, University of Gdańsk
Sobieskiego 18, 80-952 Gdańsk, Poland
Fax: (+48) 58-5235472
E-mail: janusz@raptor.chem.univ.gda.pl

[b] Prof. J. Leszczynski
Interdisciplinary Center for Nanotoxicity
Department of Chemistry, Jackson State University
Jackson, MS 39217 (USA)
Fax: (+1) 601-979-6865
E-mail: jerzy@icnanotox.org

[c] X. Li, Y. J. Ko, H. Wang, Prof. K. H. Bowen
Department of Chemistry, Johns Hopkins University
Baltimore, MD 21218 (USA)
Fax: (+1) 410-516-8420
E-mail: kbowen@jhu.edu

Supporting information for this article is available on the WWW under http://dx.doi.org/10.1002/cphc.200900810.

well below the ionization threshold of DNA can produce single- and double-strand breaks.[25] The results acquired by Sanche et al. and others[26] indicate that mainly transient anions with electrons localized on nucleobases are responsible for the observed damage. Hence, a key to comprehending the mechanism of the DNA damage seems to lie in the properties of the nucleobase, nucleoside, and nucleotide anions. For polar molecules like nucleic acid bases (NABs), dipole-bound (DB) anions exist in the gas phase.[27] However, in more complex systems (e.g., van der Waals complexes involving NABs) or in solution, valence anions are more stable than the corresponding DB species.[28]

Two main techniques are used for characterization of stable gas-phase molecular anions:[11] negative-ion photoelectron spectroscopy (PES) and Rydberg electron transfer (RET). Both methods were employed in studies concerning nucleobase valence anions.[29–32] The existence of a valence-bound state of gas-phase uracil anion has been observed by Schermann et al. by Rydberg electron-transfer spectroscopy,[29] while Weinkauf et al.[31] took advantage of the almost linear relationship between the adiabatic electron affinity (AEA) measured by photoelectron spectroscopy (PES) and the number of solvent molecules, and estimated the valence-bound (VB) AEAs of uracil and other pyrimidines by extrapolation. The cluster solvation method combined with RET spectroscopy used by Desfrancois et al.[29] also provided estimates of the valence vertical electron affinities of isolated adenine and cytosine. Recently, Bowen et al. developed a novel method of sample preparation for photoelectron spectroscopy and successfully placed all five parent NABs in the gas-phase as valence state anions.[33] The results of computational studies[34–37] revealed that the most stable valence anions of NABs are associated with so-called very rare tautomers that are formed due to N-to-C proton transfer induced by electron attachment. Furthermore, the occurrence of adiabatically stable valence anions of the parent deoxyribo- and ribonucleotides in the gas phase was recently reported by Stokes et al.[38] in PES studies. Using a novel source employing a combination of infrared desorption, electron photoemission, and gas-jet expansion they measured vertical detachment energies (VDEs) which correspond well to the results of calculations[39,40] and thus confirm the existence of adiabatically bound anionic states of the studied species.

Since most genetic material occurs in double-stranded form, interactions between electrons and base pairs seem to be far more important than the behavior of the isolated nucleobase, nucleoside, or nucleotide anions, which are too-simplified models of a complex structure. So far only two reports on stable valence anions of base pairs by combining PES measurements and theoretical calculations have been published, that is, methylated and nonmethylated adenine···thymine[41] and methylated guanine···cytosine anionic base pairs.[42] The photoelectron spectrum of the adenine···thymine (AT) base pair anion differs substantially from that of 9-methyladenine···1-methylthymine (MAMT). Although in both systems the valence anions are formed in the gas phase, the maximum of the PES feature (the VDE value) for $MAMT^{\bullet-}$ is shifted by as much as ca 0.9 eV towards lower electron binding energies (EBE) with respect to the PES of $AT^{\bullet-}$.[41] Quantum chemical calculations at the B3LYP/6-31++G(d,p) level enabled the difference between the two spectra to be ascribed to proton transfer induced by electron attachment to the lowest energy structure of the AT base pair. The Watson–Crick (WC) and Hoogsteen configurations are almost isoenergetic for the $MAMT^{\bullet-}$ anion and are characterized by the VDEs of approximately 0.8 eV that agree very well with the PES maximum.[41] In contrast, neither the WC nor the Hoogsteen arrangement is the lowest energy form of the anion of the AT base pair. Indeed, due to the absence of the methyl group at the N9 position of adenine, the most stable neutral configuration of the AT base pair is stabilized by two hydrogen bonds involving its N9 and N3 atoms. Attachment of an electron to this geometry triggers a low-energy proton transfer from N9 of adenine to O8 of thymine resulting in the valence anion with a VDE of 1.8 eV, which shifts the actual PES maximum to the high-EBE region.[41]

Herein, we report a combined experimental and theoretical study concerning the gas-phase anions of the GC base pair. Similar to the AT/MAMT case,[41] the PES spectra of the methylated, $MGMC^{\bullet-}$,[42] and unsubstituted, $GC^{\bullet-}$, base-pair anions differ substantially. While electron attachment to MAMT leads exclusively to formation of valence anions without internal proton transfer, proton transfer induced by electron attachment occurs in the unsubstituted AT system.[41] On the contrary, both the $GC^{\bullet-}$ and $MGMC^{\bullet-}$[42] valence anions exist as proton-transferred structures in the gas phase. Indeed, the PES spectrum of $MGMC^{\bullet-}$ occurs as a broad band with maximum at approximately 2.0 eV, while the GC feature consists of two bands: one of lower intensity with maximum around 2.0 eV and another with higher intensity and maximum at approximately 2.6 eV. Although the position of the first maximum in the spectrum of $GC^{\bullet-}$ corresponds well to that in the spectrum of $MGMC^{\bullet-}$, we will show in the following that the structure which is responsible for this feature is completely different from the lowest energy $MGMC^{\bullet-}$ valence anion. Moreover, we propose a mechanism which accounts for all details of the transformation leading from the lowest energy neutral GC base pair to valence anions that have VDEs reproducing very well the high-EBE feature in the PES spectrum of $GC^{\bullet-}$.

2. Results and Discussion

2.1. Photoelectron Spectrum Suggests Proton Transfer Induced by Electron Attachment to the $GC^{\bullet-}$ Anion

The broad bands in the PES spectrum of $GC^{\bullet-}$ (see Figure 1) indicate that in the gas phase these species exist as valence anions.[43] Moreover, the positions of the PES maxima in a relatively high range of EBE (a lower intensity feature with the maximum at about 2.0 eV and higher intensity peak with maximum at about 2.6 eV; see Figure 1) demonstrate that, due to electron attachment, proton transfer occurs in the studied base pairs. Indeed, it has been demonstrated in a series of experimental/computational studies[41,42,44–50] that VDEs of valence anions of nucleobases involved in complexes with various proton donors (PDs) having deprotonation energies (DPE)

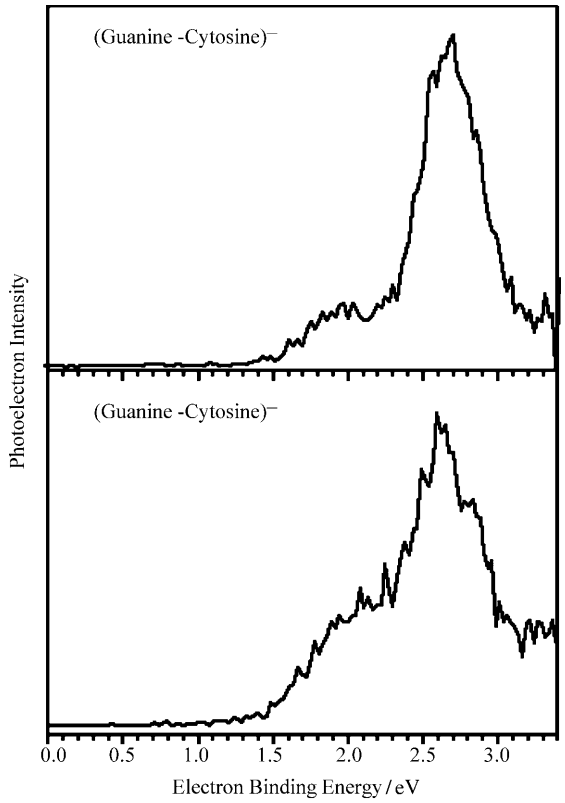

Figure 1. Photoelectron spectra of the $GC^{\bullet-}$ base-pair anions measured with 3.49 eV photons. The two spectra were recorded under two different source conditions.

sufficiently low to allow for proton transfer between PD and the NB anion fall in the range of 1.6–2.1 eV. On the other hand, if the deprotonation energy of the PD makes PT between PD and NB impossible, the VDE of an anionic complex is measured to be below 1.0 eV.[43]

2.2 Computational Interpretation of the PES Spectrum

Under the conditions employed in a photoelectron spectroscopy experiment, the gas-phase mixture of anions attains thermodynamic equilibrium.[11] Thus, the lowest (or low) energy structure(s) of the studied anions are studied experimentally. Therefore, to unravel the spectrum of the $GC^{\bullet-}$ anion one should identify the lowest energy geometry(ies) using, for instance, a reliable quantum chemistry method. A brute force method would consist of doing a complete search that would have to take into account all possible tautomers of cytosine and guanine in the configurational space of $GC^{\bullet-}$. Due to the large number of possibilities, this method does not seem to be practical (see discussion below). Another less time consuming and more elegant approach is to exploit several facts that substantially limit the configurational space of $GC^{\bullet-}$ which has to be scrutinized in order to identify the important geometries: 1) only low energy tautomers of G and C should be involved in the low energy anionic $GC^{\bullet-}$ structures, as only such tautomers are present in the neutral GC complexes which can capture an electron in the gas phase; isolated guanine and cytosine do not form stable valence anions under such conditions.[11] 2) Since the measured VDEs are located in the high-EBE region of the PES spectrum (see Figure 1), the anionic structures responsible for the high-energy peaks are those in which proton transfer between G and C occurs due to electron attachment to the GC pairs. 3) Only the low-energy neutral monohydrogenated radicals of C, $C(+H)^{\bullet}$, the products of the PT reaction within an anion of the GC base pair, are involved in the structures recorded in the PES experiment. 4) Only the low-energy closed-shell, deprotonated anions of G, $(G-H)^{-}$, the products of the PT reaction within the anion of the GC base pair, are involved in structures observed experimentally. In the following, we show that the four above-mentioned premises enable the measured PES spectrum to be unraveled within a very limited quantum chemical search through the configurational space of the $GC^{\bullet-}$ dimer.

Since the electron affinity of gaseous cytosine is substantially higher than that of guanine,[51,52] the excess electron is localized mainly on the cytosine moiety. Therefore, the proton transfer which follows electron attachment, as indicated by the relatively high EBE registered in the PES experiment (see Figure 1), should proceed in such a way that cytosine plays the role of proton acceptor, and guanine the role of proton donor in the considered PT reaction. In this connection, it is important to emphasize that although the non-PT WC GC^{-} anion is adiabatically stable,[53–57] the occurrence of a low-barrier proton transfer induced by electron attachment to nucleobase pairs involving canonical GC was demonstrated in the past in theoretical[57,58] and experimental/theoretical studies.[42]

The product of the PT reaction, a neutral monohydro radical of cytosine $C(+H)^{\bullet}$ should originate from a low-energy conformer of cytosine (see premise 1 above; for the structures of low-energy tautomers of C, see Figure 2). Therefore, in Table 1 we gathered the relative stabilities of possible monohydro radicals of cytosine $C(+H)^{\bullet}$ resulting from protonation of the valence anions of low-energy cytosine tautomers at the N or O site. The chemical structures of these monohydro radicals are shown in Figure 3. The most stable radical, Ca_N3, results from attachment of proton to the N3 site of the canonical cytosine VB anion. This structure is about 13 kcal mol^{-1} more stable, on the free enthalpy scale, than the second most stable geometry, Ca_O7_rot. Thus, the large stability difference between Ca_N3 and the remaining monohydro radicals (see Table 1) assures only Ca_N3 to be present under the experimental conditions.

The above discussion indicates that the Ca_N3 monohydro radical must be formed in the proton-transfer reaction between a low-energy tautomer of guanine (see premise 1) and the canonical cytosine anion. Therefore, one can analyze the energetics of the process leading to the GC anion by first considering the PT reaction involving the isolated substrates and products. The latter reaction can be expressed as Equation (1):

$$G_T + C^- \rightarrow G_T(-H) + Ca\_N3 \quad (1)$$

where G_T and $G_T(-H)$ stand for a low-energy tautomer of guanine and its deprotonated tautomer (closed-shell anion), respectively, while C^- and Ca_N3 (see Figure 3) are the canonical

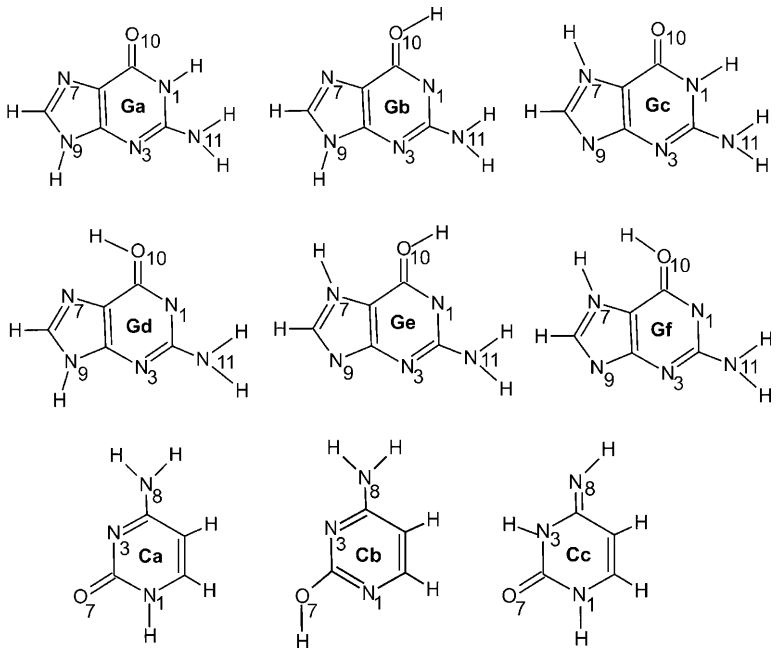

Figure 2. Chemical structures of low-energy tautomers of guanine and cytosine.

Table 1. Gas-phase basicities, G_{bas}, and their relative values, ΔG_{bas}, calculated with respect to the free energy of protonation of the canonical cytosine valence anion (C^-) at its N3 site. All values are given in kcal mol^{-1}.

Structure[a]	G_{bas}	ΔG_{bas}
Ca_N3	−343.2	0.0
Ca_O7	−322.7	20.5
Ca_O7_rot	−330.4	12.8
Cb_N3	−328.5	14.8
Cc_O7	−311.3	32.0
Cc_O7_rot	−311.8	31.5

[a] The particular entries in this column indicate the names of C^- protonation products (for their chemical structures see Figure 3).

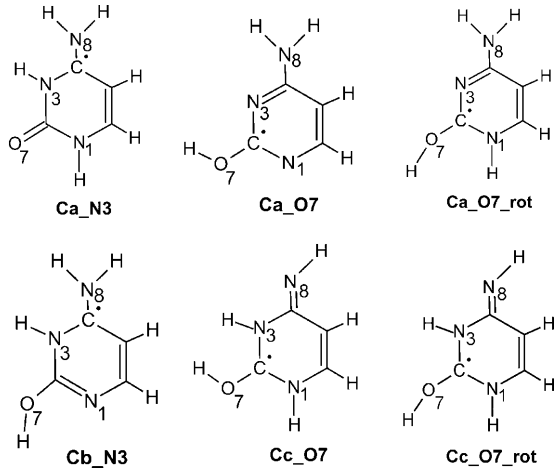

Figure 3. Chemical structures of the possible neutral monohydro radicals resulting form protonation of the anions of cytosine low energy tautomers.

cytosine anion and neutral monohydro radical of cytosine protonated at the N3 site, respectively. In such a hypothetical system, the free energy of proton transfer can be calculated as the difference between the gas-phase basicity of canonical C^- at the N3 site and the acidity of the low-energy tautomer of guanine at a chosen site. Table 2 lists acidities for the studied guanine tautomers together with the free enthalpy ΔG_{PT} of the hypothetical PT process described by Equation (1). Since we want to compare the energetics of the PT process [Eq. (1)] for different tautomers of G, the ΔG_{PT} values were corrected for the penalization energies (PEs), which stand for relative free energies of guanine tautomers calculated with regard to the most stable one, Gc (see Figure 2), resulting in ΔG_{PT}(PE) (see Table 2). To estimate PEs we employed the most accurate QCISD(T) electronic energies of guanine tautomers, published by Piacenza and Grimme,[59] and corrected them with thermal and entropy terms, calculated at the B3LYP/6-31++G(d,p) level, in order to switch from the electronic-energy to the free-enthalpy scale. The most stable GC anions should involve those G tautomers for which ΔG_{PT}(PE) assumes the most negative values. Indeed, the stability of each anionic dimer can be calculated by Equation (2) resulting from the thermodynamic cycle depicted in Figure 4 (for meaning of symbols, see the caption of Figure 4):

$$AEA_G(Y) = AEA_G(C^-) - G_{stab}[GC] + \Delta G_{PT}(PE) + G_{stab} \quad (2)$$

where ΔG_{PT}(PE) is the sum of the ΔG_{PT} and PE terms. Note that the sum of $AEA_G(C^-)$ and G_{stab}[GC] appearing in Equation (2) is constant since it involves the invariable adiabatic stability of the canonical cytosine valence anion and the stabilization free energy of the WC GC base pair. Therefore, the adiabatic stability of a base pair $AEA_G(Y)$ changes merely due to variation in the ΔG_{PT}(PE) and G_{stab} components. The ΔG_{PT}(PE) values are listed in the last column of Table 2. It is, however, not possible to predict the actual value of G_{stab} without performing QM calculations for a given anionic pair. Note that in principle a larger value of ΔG_{PT}(PE) for one of two chosen anionic pairs does not guarantee a larger value of the stabilization energy G_{stab} for that anion. Indeed, the favorable difference in ΔG_{PT}(PE) may be compensated by an unfavorable difference in G_{stab}, which could result in the anion having more negative ΔG_{PT}(PE) being less stable than the other. Therefore, in order to identify the lowest energy anionic structures one must characterize a certain set of anions with sufficiently broad range of ΔG_{PT}(PE)

Table 2. Gas-phase acidities, G_{acid}, free enthalpies of proton transfer between a low-energy tautomer of guanine and the canonical cytosine anion producing the respective closed-shell anion of guanine and the neutral monohydro radical of cytosine protonated at N3 (ΔG_{PT}), and ΔG_{PT} corrected for the penalization free energy of a given guanine tautomer [ΔG_{PT}(PE); see text for the detailed description of how the penalization free energy is calculated].[a]

Structure	G_{acid}	ΔG_{PT}	ΔG_{PT}(PE)
Ga_N1	330.9	−19.8	−19.3
Ga_N9	328.7	−22.0	−21.5
Ga_N11$_{N3}$	335.5	−15.2	−14.8
Ga_N11$_{N1}$	330.2	−20.5	−20.1
Gb_N9	330.2	−20.5	−19.8
Gb_O10	330.1	−20.5	−19.9
Gb_N11$_{N3}$	350.2	−0.5	0.1
Gb_N11$_{N1}$	349.8	−0.9	−0.2
Gc_N1	328.8	−21.9	−21.9
Gc_N7	329.2	−21.4	−21.4
Gc_N11$_{N3}$	340.2	−10.5	−10.5
Gc_N11 $_{N1}$	333.7	−17.0	−17.0
Gd_N9	327.9	−22.7	−21.7
Gd_O10	329.5	−21.1	−20.1
Gd_N11$_{N3}$	351.2	0.6	1.6
Gd_N11$_{N1}$	351.6	1.0	1.9
Ge_N7	327.5	−23.2	−19.8
Ge_O10	324.7	−25.9	−22.5
Ge_N11$_{N3}$	354.5	3.8	7.2
Ge_N11$_{N1}$	353.2	2.5	6.0
Gf_N7	320.3	−30.3	6.5
Gf_O10	317.6	−33.1	−21.9
Gf_N11$_{N3}$	347.3	−3.4	11.1
Gf_N11$_{N1}$	346.1	−4.6	7.8

[a] The symbols *x*, OY, NY, and *z* in G*x*_NY[OY]$_z$, where *x* = a, b, c, d, e or f, *Y* = 1, 7, 9, 10 or 11, and *z* = N3 or N1 (see Structure column) denote the tautomer involved in the deprotonation process or proton-transfer reaction (see Figure 2 for tautomer names), the atomic center from which a proton is detached, and which proton is detached from the amino group, respectively. For instance, Gb_N11$_{N3}$ indicates the closed-shell anion that results from detachment of the N3 side proton from the amino group of the Gb tautomer.

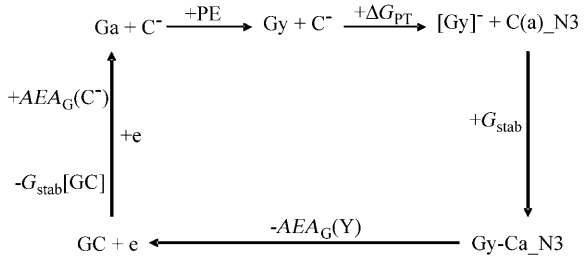

Figure 4. Thermodynamic cycle that enables the stabilities of anionic dimers to be related to the energetics of proton transfer between the isolated neutral guanine and canonical cytosine anions and the stabilization free energy of a dimer. The meaning of symbols depicted in the scheme is as follows: GC: Watson–Crick GC base pair, Ga: canonical guanine, C^-: the valence anion of canonical cytosine, $[Gy]^-$: a low-energy closed-shell anion of guanine resulting from deprotonation of the *y* tautomer, Ca_N3: monohydro radical of cytosine formed by protonation of C^- at the N3 site, Gy-Ca$_{N3}$: an anionic dimer, AEA$_G$(Y): the adiabatic electron affinity (on the free-energy scale) of Gy-Ca$_{N3}$ calculated with respect to the neutral WC GC base pair, G_{stab}[GC]: free energy of stabilization of the neutral WC GC base pair, PE: the relative free energy of tautomerization with respect to canonical guanine, ΔG_{PT}: free energy of proton transfer for isolated substrates and products, G_{stab}: free energy of stabilization of Gy-Ca$_{N3}$.

rather than limit the actual search to those geometries that are characterized by the most negative ΔG_{PT}(PE).

Recently, we published results of similar computational/experimental studies on the 9-methyguanine···1-methylcytosine base-pair anions.[42] The stabilization energies predicted for the low energy MGMC anions, that is, those that were observed in the PES experiment, differ by about 9 kcal mol^{-1}. Therefore, in the current work we focused only on those base pair anions that involve guanine anions for which ΔG_{PT}(PE) differ from the most negative value of −22.5 kcal mol^{-1} (see Table 2) by no more than 13 kcal mol^{-1}, which seems to be a safe criterion for choosing potentially the lowest energy anions of GC.

The above-described procedure allowed us to choose 15 out of 24 possible low-energy guanine closed-shell anions that could be involved in the formation of an anionic base pair (see Table 2). Another approach that, in principle, allows the photoelectron spectrum of the GC anion to be resolved utilizes a combinatorial/quantum chemistry method. However, guanine and cytosine have 36 and 12 isomers (tautomers/conformers), respectively.[60,61] If only a single dyad is created from two isomers of each set, 432 anionic structures would be possible. Additionally, every base-pair anion can form several configurations (with different hydrogen-bond networks), and additional possibilities result from the proton transfer between the VB anion of cytosine and neutral guanine. Therefore, in order to completely scrutinize the configurational space of GC$^{\bullet-}$ one would have to optimize 2000–2500 possible starting geometries (multiplication of 432 by a factor of at least 5–6 leads to 2000–2500 structures). On the other hand, the rational approach proposed in the current study reduces this enormous number of configurations to only 15 structures.

One of the most promising candidates for the lowest energy anionic GC base pair seems to be the Gf_O10 anion, characterized by ΔG_{PT} of −21.9 kcal mol^{-1}. By the same token, the least stable dimeric anion should involve Gc_N11$_{N3}$ (ΔG_{PT}(PE) = −10.5 kcal mol^{-1}; see Table 2). Indeed, data gathered in Table S1 (Supporting Information) demonstrate that this is the case (in fact, Gc$_{N11(N3)}$-Ca$_{N3}$ is the second least stable structure, but its relative free enthalpy differs by only 0.1 kcal mol^{-1} from that of the least stable, the Gc$_{N11(N1)}$-Ca$_{N3}$, anion; see Table S1 in the Supporting Information).

The B3LYP/6-31++G(d,p) geometries of the 15 anions consisting of a guanine tautomer of relatively high acidity and the Ca_N3 monohydro radical are presented in Figure 5 and Figure S1 of the Supporting Information, and their relative stabilities as well as adiabatic affinities and VDEs are gathered in Table 3 and Table S1 of the Supporting Information. The shape of the SOMO demonstrates that all of the considered structures are valence-bound anions and the excess electron is localized on the cytosine moiety (cf. beginning of discussion). As indicated by ΔG only three anionic structures can be populated in the PES experiment (see Table S1, Supporting Information): Ga$_{N1}$-Ca$_{N3}$, Gc$_{N1}$-Ca$_{N3}$, and Gf$_{O10}$-Ca$_{N3}$. The relative free energies for these structures span a range of 0-1.3 kcal mol^{-1} at the B3LYP/6-31++G(d,p) level (see Table 3). Moreover, the VDEs for these three anions can be ascribed to the maxima in the PES spectrum, that is, the VDEs of 2.02 and 2.07 eV (see

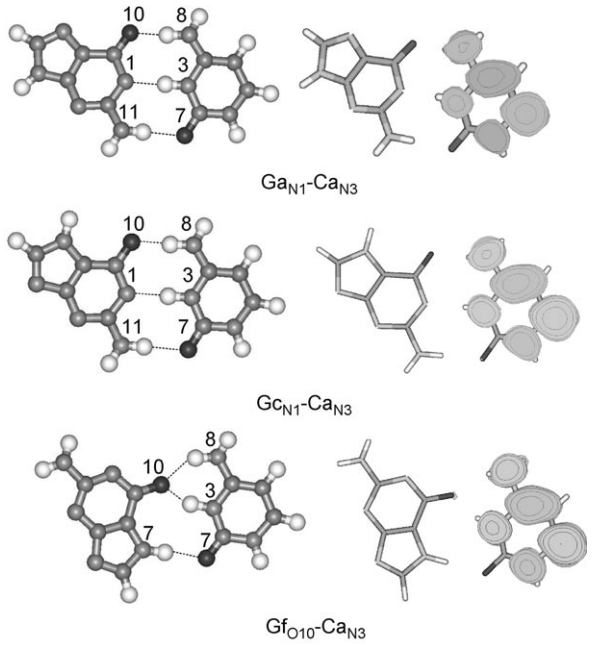

Figure 5. B3LYP/6-31++G(d,p) geometries for the three most stable anionic $(GC)^{\bullet-}$ base pairs along with their singly occupied molecular orbitals.

Table 3. Stabilization energy, E_{stab}, stabilization free energy, G_{stab}, relative stabilization free energy, ΔG_{stab}, with respect to the anionic Gf_{O10}-Ca_{N3} complex, electron vertical detachment energies (VDE), and adiabatic electron affinities (AEA) for the three most stable guanine···cytosine complexes calculated at the B3LYP/6-31++G(d,p) level. E_{stab}, G_{stab}, and ΔG_{stab} are given in kcal mol^{-1}, and VDE and AEA in eV.

Structure	E_{stab}	G_{stab}	ΔE	ΔG_{stab}[a]	AEA	VDE[b]
Ga_{N1}-Ca_{N3}	−28.8	−15.7	1.0	1.3 (2.7)	0.66	2.02 (2.23)
Gc_{N1}-Ca_{N3}	−26.5	−14.4	0.4	0.0 (0.5)	0.75	2.07 (2.31)
Gf_{O10}-Ca_{N3}	−26.9	−14.3	0.0	0.0	0.72	2.42 (2.63)

[a] The values given in brackets were calculated at the MP2/6-31++G(d,p) level (zero-point energy, thermal corrections, and entropy term were obtained at the B3LYP/6-31++G(d,p) level). [b] The values in parentheses were calculated at the B3LYP/6-31++G(d,p)//MP2/6-31++G(d,p) level.

Table 3) calculated for the Ga_{N1}-Ca_{N3} and Gc_{N1}-Ca_{N3} anions, respectively, correspond well to the first feature in the PES spectrum (see Figure 1), while the VDE of 2.42 eV calculated for Gf_{O10}-Ca_{N3} can be assigned to the second high-intensity PES peak. The latter is somewhat underestimated as compared to the experimental value of 2.6 eV. It should, however, be borne in mind that for certain systems the B3LYP method underestimates the experimentally determined VDEs.[62] This problem has been traced back to the deficiency of the B3LYP model in predicting correct geometries for some valence anions, and it turned out that the geometries of B3LYP-difficult cases are better described by the MP2 method.[62] Therefore, we did additional MP2 geometry optimizations for the three most stable structures predicted by the B3LYP model, and calculated B3LYP VDEs for their MP2 geometries [VDE(MP2)]. These VDEs move towards higher EBE region (see Table 3) as compared to those calculated consistently at the B3LYP level. The VDE(MP2) value for Gf_{O10}-Ca_{N3} is 2.63 eV (see Table 3), which remains in very good accordance with the experimental EBE of 2.6 eV. On the other hand, the VDE(MP2) values calculated for Ga_{N1}-Ca_{N3} and Gc_{N1}-Ca_{N3} somewhat overestimate the experimental maximum at 2.0 eV (see Table 3), but when corrected by the usual increment of −0.15 to −0.2 eV (the B3LYP method frequently overestimates VDEs of the anionic complexes of nucleobases by 0.15–0.2 eV) they explain the measured feature as well.

At the B3LYP level, the Gc_{N1}-Ca_{N3} and Gf_{O10}-Ca_{N3} anions are degenerate as far as their free enthalpies are concerned, while the Ga_{N1}-Ca_{N3} anion is less stable by 1.3 kcal mol^{-1} (see Table 3). As the MP2 model is more accurate than the B3LYP one, the relative stabilities predicted by the former method should be more reliable. We obtained the relative MP2 free enthalpies ΔG(MP2) of the three discussed anions by correcting their MP2/6-31++G(d,p) electronic energies with zero-point energies, thermal corrections, and entropy terms calculated at the B3LYP/6-31++G(d,p) level. Such estimated ΔG(MP2) values (see Table 3) explain the experimentally observed difference in the intensities of the two PES features. One can calculate that ΔG(MP2) of 0.5 kcal mol^{-1} (see Table 3, the relative MP2-ΔG entry for Gc_{N1}-Ca_{N3}) translates into an equilibrated system in which the content of the less stable anion Gc_{N1}-Ca_{N3} is 29% at 298 K. On the other hand, the relative free enthalpy of 2.7 kcal mol^{-1} predicted for Ga_{N1}-Ca_{N3} at the MP2 level makes this anion undetectable in the PES experiment, since at 298 K its proportion is about 0.6% of the equilibrated gas-phase mixture of anions. Hence, the two maxima observed in the PES spectrum are likely due to the presence of two isomers of $GC^{\bullet-}$, namely, Gc_{N1}-Ca_{N3} and Gf_{O10}-Ca_{N3}, in significant amounts. The former is responsible for the lower-EBE feature and the latter for the higher-EBE one.

Figure 1 shows two PES spectra obtained under different source conditions, which in principle means that the temperature of the two PES experiments was different. The observed changes of the spectrum with temperature (see Figure 1) suggest the presence of thermodynamic equilibrium in the studied system involving at least two anions with differing VDE. The relative ΔG(MP2) of 0.5 kcal mol^{-1} calculated for the Gc_{N1}-Ca_{N3} anion remains in accordance with that finding, since such small thermodynamic stimulus makes the Gc_{N1}-Ca_{N3}⇌Gf_{O10}-Ca_{N3} equilibrium temperature-sensitive. Indeed, one can calculate that, for instance, at 198 K the proportion of the Gc_{N1}-Ca_{N3} anion decreases to 14%.

Finally, a detailed picture that describes our PES experiment at the molecular level can be drawn. Initially, both constituents of the GC base pair, guanine and cytosine, are transferred to the gas phase, where they form GC base pairs. Recently, the energetic stability of 20 low-energy isomers of hydrogen-bonded GC base pair were characterized at the MP2/TZVPP level by Hobza et al.[63] Their results demonstrate that only two structures can be populated in the gas phase, namely, the Ga-Ca and Gc-Ca base pairs, both in the Watson–Crick configuration; the latter is about 1.9 kcal mol^{-1} less stable than the former.[63] Data gathered in Table 3 indicate, however, that Gc-Ca rather than Ga-Ca captures an electron, since the Gc_{N1}-Ca_{N3}

anion is more stable than the Ga_{N1}-Ca_{N3} anion (see Table 3). These two proton-transferred anions are formed immediately after electron attachment to Gc-Ca or Ga-Ca, since Gc_{N1}-Ca_{N3} and Ga_{N1}-Ca_{N3} (see Figure 6B and A) are separated by only tiny activation barriers of 0.5 and 1.0 kcal mol^{-1}, respectively, on the free-energy surface from the respective anions without PT. This is the way in which the electron-attachment process diminishes the amount of Gc-Ca in the gas-phase mixture of neutral base pairs. In order to restore the equilibrium involving the neutral species, a fraction of Ga-Ca molecules must be transformed into Gc-Ca molecules which can bind subsequent electrons. Ultimately, to attain equilibrium in the mixture of anions, Gc_{N1}-Ca_{N3} is converted to Gf_{O10}-Ca_{N3} in a low energy barrier process (6.2 kcal mol^{-1} on the free enthalpy scale, see Figure 6C) consisting of rotation of the guanine moiety by about 180° around the axis approximately defined by the C2(G) and C4(C) atoms (see Figure 6C). The transformation of Ga_{N1}-Ca_{N3} (formed from the neutral Ga-Ca base pair which dominates in the equilibrium mixture of neutrals) into Gc_{N1}-Ca_{N3} or Gf_{O10}-Ca_{N3} is not so obvious, and therefore the actual concentration of Ga_{N1}-Ca_{N3} could be larger than that resulting from the values of relative ΔG.

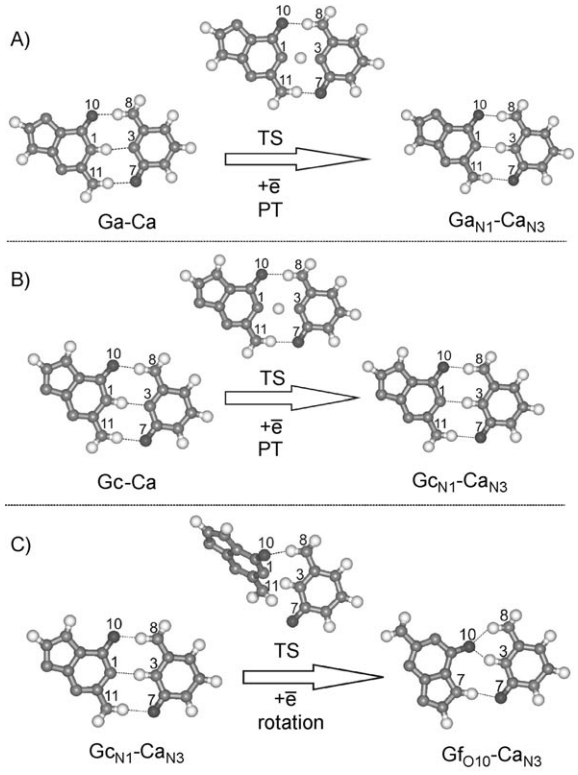

Figure 6. B3LYP/6-31++G(d,p) structures of stationary points for proton-transfer reactions Ga-Ca→Ga_{N1}-Ca_{N3} (A) and Gc-Ca→Gc_{N1}-Ca_{N3} (B) and the conformational transition (C) that leads from Gc_{N1}-Ca_{N3} to Gf_{O10}-Ca_{N3}.

3. Conclusions

A combined experimental/computational study on the electron-attachment process in guanine···cytosine (GC) base pairs reveals that adiabatically stable valence anions are formed in the gas phase. The measured VDEs of 2.0 and 2.6 eV are very well reproduced by the calculated values for the most stable anionic structures of $(GC)^{\bullet-}$ anions.

Calculations at the B3LYP/6-31++G(d,p) level were carried out for complexes comprising low-energy tautomeric forms of the studied nucleobases. In all cases an excess electron is localized on the π^* orbital of cytosine, and this leads to valence-type anions. A small difference between the relative stabilities of the two lowest energy anions, predicted by both the B3LYP and MP2 methods, suggests dependence of the PES spectrum on temperature, which was indeed observed. As in the anionic AT base pair,[41] the most populated $(GC)^{\bullet-}$ anion, Gf_{O10}-Ca_{N3}, is not biologically relevant. In both AT and GC, the lowest energy anionic structures are those in which one of the stabilizing hydrogen bonds involves a proton which is absent in the respective nucleotide (due to the N-glycosidic bond).

Given that the measured EBEs are located in the high-energy region of the PES spectrum, only proton-transferred anions were characterized computationally. Employing gas-phase basicities and acidities of low-energy tautomers of cytosine and guanine, respectively, as well as a thermodynamic cycle, we designed 15 anionic dimers of GC which could be responsible for the observed PES features. The characteristics of the three proposed structures do indeed explain the measured spectrum. The proposed computational procedure is valid for the interpretation of PES experiments carried out on any type of anionic dimers which involve tautomeric equilibria and intermolecular proton transfer. In contrast to a combinatorial approach, our procedure is much more efficient and less time consuming.

Methods Section

Experimental Details: Negative-ion photoelectron spectroscopy was conducted by crossing a mass-selected beam of anions with a fixed-frequency photon beam and energy analysis of the resultant photodetached electrons. This technique is governed by the energy-conserving relationship $hv = EKE + EBE$, where hv is the photon energy, EKE the measured electron kinetic energy, and EBE the electron binding energy. The details of our apparatus have been described elsewhere.[38,64] Briefly, both mass spectra and anion photoelectron (photodetachment) spectra were collected on an apparatus consisting of an ion source, a linear time-of-flight mass spectrometer for mass analysis and selection (resolution ca. 1000), and a magnetic-bottle photoelectron spectrometer for electron energy analysis (resolution ca. 35 meV at 1 eV EKE). The third harmonic (355 nm, 3.493 eV photon^{-1}) of a Nd:YAG laser was used to photodetach electrons from the cluster anions of interest. Photoelectron spectra were calibrated against the well-known atomic lines of the copper anion.[65] The $GC^{\bullet-}$ pair anion was generated in a novel infrared desorption/pulsed visible photoemission anion source consisting of a translating graphite bar coated with a GC mixture (ca. 50:50%), an yttrium oxide disk as photoemitter, and a pulsed gas valve to feed helium into the laser–sample interaction region. An attenuated power beam of 1064 nm light (first harmonic frequency) from a pulsed Nd:YAG laser was directed onto the graphite bar to accomplish infrared desorption. Coordinated with the IR pulses were pulses from a second Nd:YAG laser operated at

its second harmonic frequency, which were used to produce slow electrons from the photoemitter. Typically, helium gas at 4 bar was expanded in synchronization with laser pulses. Previously, this source has been utilized to successfully create parent anions of nucleosides[38] and one of the nucleotides[66] in the gas phase as well as the methylated GC (i.e., $(MGMC)^{\bullet-}$) pair anion.[42] The $GC^{\bullet-}$ pair anion was generated under similar source conditions to those that created the $(MGMC)^{\bullet-}$ pair anion, and it became the focus of the current study. By varying the source conditions, that is, by varying temperature and pressure, the relative intensities of the peaks in the photoelectron spectrum of $GC^{\bullet-}$ changed. This was not observed in the case of $(MGMC)^{\bullet-}$. An explanation of this observation was discussed in the above Results and Discussion section.

Computational Details: We applied primarily density functional theory with Becke's three-parameter hybrid functional (B3LYP)[67–69] and the 6-31++G(d,p) basis set. This level of theory has been successfully employed for other nucleobase-related systems.[43,70] All geometries presented here were fully optimized without geometrical constraints, and analysis of harmonic frequencies proved that all of them are either structures at energetic minima (all force constants positive) or first-order transition points (all but one force constants positive). The stabilization energies E_{stab} of the anionic complexes are calculated as the difference between the energy of the complex and the sum of the energies of fully optimized isolated monomers, that is, a closed-shell anion of deprotonated guanine and the open-shell (doublet) monohydro radical of cytosine. In addition to the stabilization energies E_{stab}, we also calculated the stabilization free energies G_{stab}. The latter is determined by correcting the values of E_{stab} for zero-point vibration, thermal contributions to energy, the pV term, and the entropy term. These terms were calculated in the rigid rotor/harmonic oscillator approximation for $T = 298$ K and $p = 1$ atm. Electron vertical detachment energies, direct observables in the PES experiment, were evaluated as differences between the energy of the neutral and anionic complex at the geometry of the fully relaxed anion. The difference in Gibbs free energies of neutral Watson–Crick GC and an anion at their corresponding fully relaxed geometries is denoted AEA_G.

To refine the QM description of the three lowest energy anionic structures we carried out additional MP2/6-31++G(d,p) geometry optimizations. The relative stabilities of particular anions were obtained by using the PMP2 energies. The 1s core orbitals of carbon, nitrogen, and oxygen were excluded from the MP2 treatment.

All quantum chemical calculations were carried out with the Gaussian 03[67] code, and pictures of molecular orbitals were plotted with the MOLDEN package.[68]

Acknowledgements

This work was partially supported by the Polish Ministry of Science and Higher Education (MNiSW), Grant No. NN204 125537 (A.S.) and NN204 023135 (J.R), ONR Grant (N00034-03-1-0116) and NSF CREST Grant No. HRD-0318519 (J.L.), and The US National Science Foundation under Grant No. CHE-0809258 (K.B.). The calculations were performed at the Academic Computer Center in Gdańsk (TASK) and the Mississippi Center for Supercomputing Research.

Keywords: density functional calculations · nucleobases · photoelectron spectroscopy · proton transfer · radical ions

[1] D. D. Eley, D. I. Spivey, *Trans. Faraday Soc.* **1962**, *58*, 411–415.
[2] C. Wan, T. Fiebig, S. O. Kelley, C. R. Treadway, J. K. Barton, A. H. Zewail, *Proc. Natl. Acad. Sci. USA* **1999**, *96*, 6014–6019.
[3] T. Takada, K. Kawai, X. Cai, A. Sugimoto, M. Fujitsuka, T. Majima, *J. Am. Chem. Soc.* **2004**, *126*, 1125–1129.
[4] F. D. Lewis, H. Zhu, P. Daublain, B. Cohen, M. R. Wasielewski, *Angew. Chem.* **2006**, *118*, 8150–8153; *Angew. Chem. Int. Ed.* **2006**, *45*, 7982–7985.
[5] D. B. Hall, R. E. Holmlin, J. K. Barton, *Nature* **1996**, *382*, 731–735.
[6] M. E. Nunez, D. B. Hall, J. K. Barton, *Chem. Biol.* **1999**, *6*, 85–97.
[7] D. Ly, L. Sanii, G. B. Schuster, *J. Am. Chem. Soc.* **1999**, *121*, 9400–9410.
[8] K. Nakatani, S. Sando, I. Saito, *J. Am. Chem. Soc.* **2000**, *122*, 2172–2177.
[9] R. E. Holmlin, P. J. Dandliker, J. K. Barton, *Angew. Chem.* **1997**, *109*, 2830–2848; *Angew. Chem. Int. Ed. Engl.* **1997**, *36*, 2714–2730.
[10] P. J. Dandliker, R. E. Holmlin, J. K. Barton, *Science* **1997**, *275*, 1465–1468.
[11] D. Svozil, P. Jungwirth, Z. Havlas, *Collect. Czech. Chem. Commun.* **2004**, *69*, 1395–1428.
[12] H. W. Fink, C. Schönenberger, *Nature* **1999**, *398*, 407–410.
[13] H. W. Fink, *Cell. Mol. Life Sci.* **2001**, *58*, 1–3.
[14] N. Robertson, C. A. McGowan, *Chem. Soc. Rev.* **2003**, *32*, 96–103.
[15] T. Carell, C. Behrens, J. Gierlich, *Org. Biomol. Chem.* **2003**, *1*, 2221–2228.
[16] M. A. O'Neill, J. K. Barton in *Charge Transfer in DNA: From Mechanism to Application* (Eds.: H. A. Wagenknecht), Wiley, New York, **2005**, pp. 27–75.
[17] G. B. Schuster, *Acc. Chem. Res.* **2000**, *33*, 253–260.
[18] B. Giese in *Topics in Current Chemistry: Long-Range Charge Transfer in DNA I*, (Ed.: G. B. Schuster), Springer-Verlag, Berlin/Heidelberg, **2004**, 236, pp. 27–44.
[19] B. Giese, B. Carl, T. Carl, T. Carell, C. Behrens, U. Hennecke, O. Schiemann, E. Feresin, *Angew. Chem.* **2004**, *116*, 1884–1887; *Angew. Chem. Int. Ed.* **2004**, *43*, 1848–1851.
[20] S. Breeger, U. Hennecke, T. Carell, *J. Am. Chem. Soc.* **2004**, *126*, 1302–1303.
[21] C. Haas, K. Kräling, M. Cichon, N. Rahe, T. Carell, *Angew. Chem.* **2004**, *116*, 1878–1880; *Angew. Chem. Int. Ed.* **2004**, *43*, 1842–1844.
[22] C. Behrens, T. Carell, *Chem. Commun.* **2003**, 1632–1633.
[23] T. Ito, S. E. Rokita, *J. Am. Chem. Soc.* **2004**, *126*, 15552–15559.
[24] M. Tanaka, K. Ohkubo, S. Fukuzumi, *J. Am. Chem. Soc.* **2006**, *128*, 12372–12373.
[25] B. Boudaiffa, P. Cloutier, D. Hunting, M. A. Huels, L. Sanche, *Science* **2000**, *287*, 1658–1660.
[26] L. Sanche, *Eur. Phys. J. D* **2005**, *35*, 367–390.
[27] N. A. Oyler, L. Adamowicz, *J. Phys. Chem.* **1993**, *97*, 11122–11123.
[28] M. D. Sevilla, B. Besler, A. O. Colson, *J. Phys. Chem.* **1994**, *98*, 2215.
[29] C. Desfrançois, V. Periquet, Y. Bouteiller, J. P. Schermann, *J. Phys. Chem. A* **1998**, *102*, 1274–1278.
[30] J. H. Hendricks, S. A. Lyapustina, H. L. de Clercq, J. T. Snodgrass, K. H. Bowen, *J. Chem. Phys.* **1996**, *104*, 7788–7791.
[31] J. Schiedt, R. Weinkauf, D. M. Neumark, E. W. Schlag, *Chem. Phys.* **1998**, *239*, 511–524.
[32] V. Periquet, A. Moreau, S. Carles, J. P. Schermann, C. Desfrançois, *J. Electron. Spectrosc. Relat. Phenom.* **2000**, *106*, 141–151.
[33] X. Li, K. H. Bowen, M. Haranczyk, R. A. Bachorz, K. Mazurkiewicz, J. Rak, M. Gutowski, *J. Chem. Phys.* **2007**, *127*, 174309/1–174309/6.
[34] M. Haranczyk, M. Gutowski, X. Li, K. H. Bowen, *Proc. Natl. Acad. Sci. USA* **2007**, *104*, 4804–4807.
[35] M. Haranczyk, M. Gutowski, *Angew. Chem.* **2005**, *117*, 6743–6746; *Angew. Chem. Int. Ed.* **2005**, *44*, 6585–6588.
[36] M. Haranczyk, M. Gutowski, *J. Am. Chem. Soc.* **2005**, *127*, 699–706.
[37] R. A. Bachorz, J. Rak, M. Gutowski, *Phys. Chem. Chem. Phys.* **2005**, *7*, 2116–2125.
[38] S. T. Stokes, X. Li, A. Grubisic, Y. J. Ko, K. H. Bowen, *J. Chem. Phys.* **2007**, *127*, 084321/1–084321/6.
[39] N. A. Richardson, J. Gu, S. Wang, Y. Xie, H. F. Schaefer III, *J. Am. Chem. Soc.* **2004**, *126*, 4404–4411.
[40] X. Li, L. Sanche, M. D. Sevilla, *Radiat. Res.* **2006**, *165*, 721–729.
[41] D. Radisic, K. H. Bowen, I. Dąbkowska, P. Storoniak, J. Rak, M. Gutowski, *J. Am. Chem. Soc.* **2005**, *127*, 6443–6450.
[42] A. Szyperska, J. Rak, J. Leszczynski, X. Li, Y. J. Ko, H. Wang, K. H. Bowen, *J. Am. Chem. Soc.* **2009**, *131*, 2663–2669.

[43] J. Rak, K. Mazurkiewicz, M. Kobyłecka, P. Storoniak, M. Harańczyk, I. Dąbkowska, R. A. Bachorz, M. Gutowski, D. Radisic, S. T. Stokes, S. N. Eustis, D. Wang, X. Li, Y. J. Ko, K. H. Bowen in *Radiation Induced Molecular Phenomena in Nucleic Acids: A Comprehensive Theoretical and Experimental Analysis* (Eds.: M. K. Shukla, J. Leszczynski), Springer-Verlag, Amsterdam, **2008**, pp. 619 – 667.
[44] M. Harańczyk, R. A. Bachorz, J. Rak, M. Gutowski, D. Radisic, S. T. Stokes, J. M. Nilles, K. H. Bowen, *J. Phys. Chem. B* **2003**, *107*, 7889 – 7895.
[45] M. Gutowski, I. Dąbkowska, J. Rak, S. Xu, J. M. Nilles, D. Radisic, K. H. Bowen, Jr., *Eur. Phys. J. D* **2002**, *20*, 431 – 439.
[46] M. Haranczyk, J. Rak, M. Gutowski, D. Radisic, S. T. Stokes, J. M. Nilles, K. H. Bowen, *Isr. J. Chem.* **2004**, *44*, 157 – 170.
[47] M. Harańczyk, I. Dąbkowska, J. Rak, M. Gutowski, J. M. Nilles, S. T. Stokes, D. Radisic, K. H. Bowen, *J. Phys. Chem. B* **2004**, *108*, 6919 – 6921.
[48] I. Dąbkowska, J. Rak, M. Gutowski, J. M. Nilles, D. Radisic, K. H. Bowen, Jr., *J. Chem. Phys.* **2004**, *120*, 6064 – 6071.
[49] I. Dąbkowska, J. Rak, M. Gutowski, D. Radisic, S. T. Stokes, J. M. Nilles, K. H. Bowen, Jr., *Phys. Chem. Chem. Phys.* **2004**, *6*, 4351 – 4357.
[50] M. Harańczyk, J. Rak, M. Gutowski, D. Radisic, S. T. Stokes, K. H. Bowen, *J. Phys. Chem. B* **2005**, *109*, 13 383 – 13 391.
[51] M. D. Sevilla, B. Besler, A. O. Colson, *J. Phys. Chem.* **1995**, *99*, 1060 – 1063.
[52] X. Li, Z. Cai, M. D. Sevilla, *J. Phys. Chem. A* **2002**, *106*, 1596 – 1603.
[53] A. Kumar, M. Knapp-Mohammady, P. C. Mishra, S. Suhai, *J. Comput. Chem.* **2004**, *25*, 1047 – 1059.
[54] A. O. Colson, B. Besler, D. M. Close, M. D. Sevilla, *J. Phys. Chem.* **1992**, *96*, 661 – 668.
[55] J. Smets, A. F. Jalbout, L. Adamowicz, *Chem. Phys. Lett.* **2001**, *342*, 342 – 346.
[56] N. A. Richardson, S. S. Wesolowski, H. F. Schaefer III, *J. Am. Chem. Soc.* **2002**, *124*, 10163 – 10170.
[57] X. Li, Z. Cai, M. D. Sevilla, *J. Phys. Chem. B* **2001**, *105*, 10115 – 10123.
[58] J. Gu, Y. Xie, H. F. Schaefer III, *J. Chem. Phys.* **2007**, *127*, 155107/1 – 155107/6.
[59] M. Piacenza, S. Grimme, *J. Comput. Chem.* **2004**, *25*, 83 – 99.
[60] W. Liang, H. Li, X. Hu, S. Han, *Chem. Phys.* **2006**, *328*, 93 – 102.
[61] G. Fogarasi, *J. Phys. Chem. A* **2002**, *106*, 1381 – 1390.
[62] K. Mazurkiewicz, M. Harańczyk, M. Gutowski, J. Rak, D. Radisic, S. N. Eustis, D. Wang, K. H. Bowen, *J. Am. Chem. Soc.* **2007**, *129*, 1216 – 1224.
[63] A. Abo-Riziq, L. Grace, E. Nir, M. Kabelac, P. Hobza, M. S. de Vries, *Proc. Natl. Acad. Sci. USA* **2005**, *102*, 20 – 23.
[64] O. C. Thomas, W. J. Zheng, K. H. Bowen, *J. Chem. Phys.* **2001**, *114*, 5514 – 5519.
[65] R. C. Bilodeau, M. Scheer, H. K. Haugen, *J. Phys. B* **1998**, *31*, 3885 – 3891.
[66] S. T. Stokes, A. Grubisic, X. Li, Y. J. Ko, K. H. Bowen, *J. Chem. Phys.* **2008**, *128*, 044314/1 – 044314/5.
[67] A. D. Becke, *Phys. Rev. A* **1988**, *38*, 3098 – 3100.
[68] A. D. Becke, *J. Chem. Phys.* **1993**, *98*, 5648 – 5652.
[69] C. Lee, W. Yang, R. G. Parr, *Phys Rev. B* **1988**, *37*, 785 – 789.
[70] J. C. Rienstra-Kiracofe, G. S. Tschumper, H. F. Schaefer III, S. Nandi, G. B. Ellison, *Chem. Rev.* **2002**, *102*, 231 – 282.
[71] Gaussian 03, Revision B.05, M. J. Frisch, G. W. Trucks, H. B. Schlegel, G. E. Scuseria, M. A. Robb, J. R. Cheeseman, J. A. Montgomery, Jr., T. Vreven, K. N. Kudin, J. C. Burant, J. M. Millam, S. S. Iyengar, J. Tomasi, V. Barone, B. Mennucci, M. Cossi, G. Scalmani, N. Rega, G. A. Petersson, H. Nakatsuji, M. Hada, M. Ehara, K. Toyota, R. Fukuda, J. Hasegawa, M. Ishida, T. Nakajima, Y. Honda, O. Kitao, H. Nakai, M. Klene, X. Li, J. E. Knox, H. P. Hratchian, J. B. Cross, C. Adamo, J. Jaramillo, R. Gomperts, R. E. Stratmann, O. Yazyev, A. J. Austin, R. Cammi, C. Pomelli, J. W. Ochterski, P. Y. Ayala, K. Morokuma, G. A. Voth, P. Salvador, J. J. Dannenberg, V. G. Zakrzewski, S. Dapprich, A. D. Daniels, M. C. Strain, O. Farkas, D. K. Malick, A. D. Rabuck, K. Raghavachari, J. B. Foresman, J. V. Ortiz, Q. Cui, A. G. Baboul, S. Clifford, J. Cioslowski, B. B. Stefanov, G. Liu, A. Liashenko, P. Piskorz, I. Komaromi, R. L. Martin, D. J. Fox, T. Keith, M. A. Al-Laham, C. Y. Peng, A. Nanayakkara, M. Challacombe, P. M. W. Gill, B. Johnson, W. Chen, M. W. Wong, C. Gonzalez, J. A. Pople, Gaussian, Inc., Pittsburgh, PA, **2003**.
[72] G. Schaftenaar, J. H. Noordik, *J. Comput. Aided. Mol. Des.* **2000**, *14*, 123 – 134.

Received: October 15, 2009
Published online on February 2, 2010

